



Published in final edited form as:

IEEE Trans Neural Syst Rehabil Eng. 2008 April ; 16(2): 195–204. doi:10.1109/TNSRE.2008.918425.

A Model of Selective Activation of the Femoral Nerve With a Flat Interface Nerve Electrode for a Lower Extremity Neuroprosthesis

Matthew A. Schiefer [Student Member, IEEE],

Department of Biomedical Engineering, Case Western Reserve University, Cleveland, OH 44106 USA, Louis Stokes Department of Veterans Affairs Medical Center, Cleveland, OH 44106 USA

Ronald J. Triolo [Member, IEEE], and

Departments of Biomedical Engineering and Orthopaedics, Case Western Reserve University, Cleveland, OH 44106 USA, Louis Stokes Department of Veterans Affairs Medical Center, Cleveland, OH 44106 USA

Dustin J. Tyler [Member, IEEE]

Department of Biomedical Engineering, Case Western Reserve University, Cleveland, OH 44106 USA, Louis Stokes Department of Veterans Affairs Medical Center, Cleveland, OH 44106 USA

Matthew A. Schiefer: matthew.schiefer@case.edu; Ronald J. Triolo: ronald.triolo@case.edu; Dustin J. Tyler: dustin.tyler@case.edu

Abstract

Functional electrical stimulation (FES) can restore limb movements through electrically initiated, coordinated contractions of paralyzed muscles. The peripheral nerve is an attractive site for stimulation using cuff electrodes. Many applications will require the electrode to selectively activate many smaller populations of axons within a common nerve trunk. The purpose of this study is to computationally model the performance of a flat interface nerve electrode (FINE) on the proximal femoral nerve for standing and stepping applications. Simulations investigated multiple FINE configurations to determine the optimal number and locations of contacts for the maximum muscular selectivity. Realistic finite element method (FEM) models were developed from digitized cross sections from cadaver femoral nerve specimens. Electrical potentials were calculated and interpolated voltages were applied to a double-cable axon model. Model output was analyzed to determine selectivity and estimate joint moments with a musculoskeletal model. Simulations indicated that a 22-contact FINE will produce the greatest selectivity. Simulations predicted that an eight-contact FINE can be expected to selectively stimulate each of the six muscles innervated by the proximal femoral nerve, producing a sufficient knee extension moment for the sit-to-stand transition and contributing 60% of the hip flexion moment needed during gait. We conclude that, whereas more contacts produce greater selectivity, eight channels are sufficient for standing and stepping with an FES system using a FINE on the common femoral nerve.

Index Terms

Electrode; femoral nerve; flat interface nerve electrode (FINE); functional electrical stimulation (FES); selective stimulation

I. Introduction

Between 250 000 and 450 000 Americans are living with spinal cord injuries (SCIs). There are 11 000 new injuries annually. SCI results in partial or complete loss of function and sensation below the level of injury [1]–[3]. Functional electrical stimulation (FES) can restore limb movements through electrically initiated, coordinated contractions of paralyzed muscles. Implanted neuroprostheses employing epimysial and intramuscular electrodes have restored short duration standing and stepping function to select individuals with paraplegia [4]–[6]. These muscle-based systems can be highly selective in activating the muscles required for a desired motion by positioning the stimulating electrodes in or on the targeted muscle motor end plate. However, this requires separate surgical approaches for deploying an electrode on each muscle and may result in only partial recruitment of large muscles with multiple motor end plates [7]. Nerve-based electrodes, such as a cuff electrode on the common femoral nerve, are an alternative to muscle-based electrodes.

Because the proximal femoral nerve is broad and flat, the flat interface nerve electrode (FINE) is an attractive choice to take advantage of the existing geometric organization of fascicles for selective activation of the axons serving the vastus lateralis, vastus medialis, and vastus intermedius (knee extension), the rectus femoris (knee extension, hip flexion), the sartorius (hip and knee flexion), and the pectineus (hip flexion). Animal experiments have shown that the FINE can selectively restore individual functions controlled by a single nerve [8]–[10]. The morphology of nerves in the animal model differs from the human. In the animal, nerves contain a smaller number of fascicles. The human femoral nerve, however, contains a large number of fascicles of which multiple fascicles contain axons innervating a single muscle.

Selective stimulation is important because different functions (knee extension or hip flexion) are required during different phases of gait. In addition, selective stimulation of the vasti may be used for interleaved activation of synergistic muscles to delay the onset of fatigue [11]. This is particularly important when supporting the body weight of taller or heavier individuals. A nerve-based approach offers the potential of fully recruiting all axons innervating a targeted muscle, thus increasing its stimulated force output and the joint moment available. Further, a single selective multicontact nerve cuff electrode positioned proximally could reduce surgery time by requiring only a single implant for multiple functions.

The hypothesis of this study is that a FINE placed proximally on the common femoral nerve (translucent ellipse in Fig. 1(a) with a fixed number of contacts at predetermined locations and without *a priori* knowledge of the nerve's fascicular microstructure can selectively activate each muscle innervated by the femoral nerve and produce adequate moments for standing and stepping using only a simple monopolar, square, cathodic stimulating waveform. Through the use of finite element models, nonlinear axonal models, and biomechanical models, this simulation study investigates multiple FINE opening heights and multicontact configurations to optimize the number and locations of contacts to produce the selectivity necessary for standing and stepping. A value of 0.4 Nm/kg (or 40 Nm for a 100 kg individual) has been reported to be sufficient to produce a large enough knee extension moment for the sit-to-stand transfer [12], [13]. A value of 0.3 Nm/kg (or 30 Nm for a 100 kg individual) has been reported to be sufficient to produce a large enough hip flexion moment for normal gait [14], [15]. Nerve simulations are based on actual geometry and fascicular distribution within the common femoral nerve derived from quantitative anatomical studies.

II. Methods

Realistic finite element models of proximal human femoral nerves and FINEs were created from histology of the cross sections from three cadavers [Fig. 1(b)] [16]. The nerves contained 47, 25, and 22 fascicles, respectively. Images of human femoral nerve cross sections approximately 10 mm distal to the inguinal ligament were imported into AutoCAD 2000 (Autodesk, San Rafael, CA). Borders of the epineurium and endoneurium were traced and the 2-D image was imported into Maxwell 3D V10 (Ansoft, Pittsburgh, PA). In Maxwell, the perineurium of each fascicle was added as a tissue layer surrounding each endoneurium. Perineurial thickness was set to 3% of the fascicular diameter [17]. To simulate the intra-operative environment, the space between the electrode and the nerve was modeled as saline. Fascicles and the epineurium were extruded to create a “semi-infinite” 3-D finite element method (FEM) model. Voltages within the nerve for a model extruded 60 mm differed by less than 1% from a 500 mm model and required only 10.5% of the time to solve. These data were unaffected by ground boundary conditions set on the edges of a 150 mm 150 mm 200 mm saline volume. The maximum current density on all edges of the saline was at least six orders of magnitude less than the maximum current density within the electrode. The 60 mm models represented an infinite system. The tissue properties used are detailed in Table I.

A FINE was modeled in Maxwell 3-D as a rectangular silicone cuff around the femoral nerve [Fig. 2(a)]. The FINE was 10 mm in length along the nerve and 11.8 mm wide, which was slightly larger than the widest nerve cross section. The wall thickness of the FINE was 0.6 mm. Contact stimulating surfaces were 0.5 mm \times 0.5 mm and spaced 1.0 mm on-center [18]. A total of 22 platinum contacts (11 on top and 11 on bottom) were simulated. This was chosen as the maximum number of contacts that can be built with present fabrications techniques for clinical trials. Since the number of stimulus channels in an implanted system is limited, the electrode with the fewest contacts to produce the required function is preferred. To examine the minimum number of contacts, several electrode configurations were studied (Table II).

Configurations 11_A and 11_B contained 11 contacts on only the upper or lower interior surface of the electrode, respectively. This represented a 50% reduction in the total number of contacts. The “B” configuration was a compliment to the “A” configuration and corresponded to the situation where the “A” electrode is placed on the nerve backwards or upside down. Configurations and contained 8 contacts: 4 on the upper and 4 on the lower surface. Contacts in these configurations were staggered so that those on one surface were located in between those on the opposite surface. Configurations and contained 6 contacts: 3 on the upper surface and 3 on the lower surface. Six contacts produced a 1:1 ratio between the number of contacts and number of targeted muscles. This represented the theoretical minimum number of contacts required to selectively stimulate each muscle with simple, single channel, monopolar stimulation. Configurations 8_C and 6_C contained 8 and 6 contacts, respectively, with contacts located symmetrically at or near the center of the cuff and at the outer edges of the cuff thereby maintaining the same spatial position relative to any fascicle within the nerve regardless of orientation of the electrode on the nerve. This configuration was hypothesized to take advantage of the distribution of fascicles to the knee extensors located toward the center of the nerve and fascicles to the hip flexors located toward the medial or lateral edges of the nerve [Fig. 1(b)]. This pattern was consistent in all nerves studied.

FINE opening heights of 3.8, 2.3, and 1.4 mm were modeled. These represented negligible/no nerve reshaping, slight nerve reshaping with less than 5% of the fascicles of any cross section being redistributed, and moderate nerve reshaping, respectively [Fig. 2(b)]. Fascicles

were assumed to move, but not change shape, though this has been demonstrated in animal trials [18]. For models in which fascicles were moved, fascicles were algorithmically shifted inward parallel to the short axis, toward the center of the nerve starting with the fascicle farthest from the long axis of the nerve. If a shifting fascicle touched another fascicle, the shifting fascicle was shifted medially or laterally to avoid overlap.

Maxwell 3-D calculated electrical potentials induced by a 1 mA cathodic input current at a contact. The potentials were exported to MATLAB V7 (The Mathworks, Inc., Natick, MA), where the voltages along axons were interpolated using a 3-D cubic spline. Axons with varying diameters were randomly and uniformly distributed throughout each fascicle. Since the distribution of axon diameters within the femoral nerve is unknown, the known distribution of fiber diameters for human sensory fibers in the sural nerve [19] and human motor fibers in the tibial nerve [20] were used for sensory and motor fascicles, respectively. The offset of the central Node of Ranvier, defined as the Node closest to the center of the stimulating electrode, was randomly varied between 0 mm (the node was directly beneath the electrode) and half of the axon's internodal length.

Voltages were interpolated for the nodes and internodes of each axon and exported to NEURON (Hines, Moore, and Carnevale¹) where they were applied as an extracellular field to the a double cable axon model to represent the mammalian motor axon response to external stimulation [21], [22]. This model included persistent and fast sodium, slow potassium, and leakage currents in the Nodes of Ranvier. Simulations were run in NEURON for all combinations of pulse widths of 0.02, 0.05, 0.10, 0.20, 0.50, 1.00, 2.00, 5.00, and 10.00 ms and pulse amplitudes of 0.10, 0.20, 0.50, 1.00, and 2.00 mA.

Results from these simulations were analyzed in MATLAB to determine which contacts produced the greatest selectivity. Adapted from Choi *et al.* [23], muscular selectivity, S_{muscle} , was defined as the fraction of axons activated within all fascicles innervating a target muscle (the "recruitment benefit" or "RB") minus the fraction of axons not innervating the target muscle that were activated (the "recruitment cost" or "RC") (Fig. 3). For each electrode configuration, the maximum selectivity produced for each muscle in each model was calculated for 1) a single contact to selectively stimulate a muscle [(1) 6930 total permutations] and 2) a combination of two contacts to selectively stimulate a muscle [(2), 3 586 275 total permutations). Results from simulations in which two contacts were chosen for selective stimulation of a muscle ("choose-2") were compared to those obtained from single contact simulations ("choose-1")

$$S_{\text{muscle}} = RB_c - RC_c \quad (1)$$

$$S_{\text{muscle}} = [(RB_{c_1} + RB_{c_2} - RRB_{c_1, c_2}) - (RC_{c_1} + RC_{c_2} - RRC_{c_1, c_2})] \quad (2)$$

$$\forall c_1, c_2 \in C \wedge c_1 \neq c_2.$$

In (2), c_1 and c_2 were unique contacts $\in \{1, 2\}$. Axon recruitment with the two contacts was considered independent, as would occur with delayed or nonoverlapping stimulation. RRB and RRC were redundancy terms associated with the recruitment benefit and recruitment cost obtained from overlapping fields from multiple contacts, respectively. Subtraction of these terms accounted for axons that were activated by both contacts.

¹<http://www.neuron.yale.edu>

Equations (1) and (2) produced values ranging from -1.0 to 1.0 . A selectivity value of 1.0 indicated that 100% of target axons were activated while 0% of nontarget axons were activated, whereas a value of -1.0 indicated that 0% of target axons were activated while 100% of nontarget axons were activated. Activation of sensory fascicles (serving medial cutaneous and saphenous nerves) always contributed to the recruitment costs even though their recruitment would not adversely affect an individual with a neurologically complete SCI, thus underestimating the useful selectivity that may be expected during clinical application in SCI.

An additional optimization constraint considered was to require the recruitment costs associated with all nontarget fascicle groups to be less than 10% . A 10% recruitment has been indicated as an activation threshold below which a muscle force can be considered negligible [9], [24]. If it was not possible to selectively stimulate a target fascicle group without stimulating more than 10% of any nontarget fascicle group then the selectivity value was defined as zero.

To estimate the functional outcome, the activation level of each muscle was used to estimate resulting knee and hip moments using a biomechanical model. Simulations using the seven segment kinematic model of the lower extremity developed by Delp [25], [26] were implemented in SIMM (Software for Interactive Musculoskeletal Modeling, Musculographics, Inc., Santa Rosa, CA) to find the maximum isometric moments that each muscle innervated by the femoral nerve could exert at the knee and hip. This model has been detailed elsewhere [25]–[29]. Since joint moment is dependent on hip and knee angles, simulations of both the sitting and standing positions were performed. The model output was four moments associated with each muscle: the moment produced at the knee when the knee was 1) flexed at 90° during sitting or 2) extended at 0° during standing and the moment produced at the hip when the hip was 3) flexed at 90° during sitting or 4) extended at 0° during standing (Table III). Contraction dynamics were ignored and only steady state moments were recorded. Percent activation of a muscle was assumed to be directly proportional to the fraction of axons innervating a muscle that was activated during stimulation. Therefore, maximum isometric muscle forces were simply scaled by the axonal activation level for each muscle. The isometric joint moments produced by the six muscles in the system were summed to determine the cumulative knee extension and hip flexion moments. Joint moments were reported as ranges due to the variation in moment over the joint angles tested. The cumulative knee extension and hip flexion moments were compared to published values to determine if the selectivity obtained during stimulation was sufficient to produce a large enough moment for the sit-to-stand transfer and for normal gait.

All FEM simulations and MATLAB analyses were run on a workstation with an AMD Athlon 64 FX-53 processor with 4 GB of RAM or a workstation housing two dual-core AMD Opteron 280 processors with 2 GB of RAM per core. NEURON simulations were conducted remotely at the Ohio Supercomputer Center's P4 cluster. NEURON simulations were run in parallel to minimize total computation time. The results obtained with the 22-contact model (the control) and all other models with random axon distributions were compared using paired one-tailed t-tests. For all statistical tests, an acceptance level of $\alpha = 0.05$ was used. Bonferroni adjustments were used to account for multiple comparisons [30].

III. Results

A. Simulation Performance

Ansoft Maxwell v.10 calculated voltage distributions in 66 ± 46 minutes per contact. Simulation time increased as FINE opening height decreased as this typically required more nodal elements. MATLAB interpolated the voltages along randomly positioned axons at a

rate of 0.38 ms per Node of Ranvier. NEURON simulated all axons at all stimulation parameters at an approximate rate of 10 days/cross section/opening height (23.859 M axons were simulated in total).

B. Performance of the 22-Contact Fine

The 22-contact FINE (control) produced the greatest selectivity under all tested scenarios. When using a single contact, selectivity values ranged from the lowest of 0.11 ± 0.05 when targeting the vastus lateralis with a 3.8 mm FINE to the highest of 0.74 ± 0.08 when targeting the pectineus with a 2.3 mm FINE (Table IV). The selectivity obtained for all muscles with the 2.3 mm FINE was significantly greater in four of the six muscles than that obtained for the 3.8 mm FINE ($p \leq 0.05$). No significant difference was seen for the vastus lateralis ($p = 0.11$) and sartorius ($p = 0.58$). The 2.3 mm FINE had a higher fraction of activated target axons (RB) and a smaller fraction of spillover (RC) than for the 3.8 mm FINE. The selectivity obtained with the 1.4 mm FINE was not significantly greater than that obtained with the 2.3 mm FINE for five out of six muscles. It was significantly higher for the sartorius muscle ($p \leq 0.05$).

Simultaneous stimulation of two heads of the vasti with two independent contacts while in a seated posture resulted in a knee extension moment of at least 40 Nm for all 22-contact FINE opening heights (Fig. 4). Hip flexion moment was negligible when selectively stimulating any of the vasti for all electrode opening heights. Selective stimulation of the sartorius and the pectineus in a standing posture produced hip flexion moments of 6 ± 1 Nm with negligible knee extension moments due to spillover. In a seated posture, selective stimulation of the rectus femoris resulted in a 13 ± 1 Nm hip flexion moment and a 17 ± 0 Nm knee extension moment. In a standing posture, selective stimulation of the rectus femoris resulted in a 15 ± 2 Nm hip flexion moment and a 26 ± 0 Nm knee extension moment. Simultaneous, selective stimulation of all hip flexors in a standing posture produced 21 ± 2 Nm of hip flexion, or 70% of the required 30 Nm hip flexion moment for gait.

The 22-contact FINE was able to selectively activate each muscle above threshold without activating any other muscle above threshold in 40 of 42 (95%) modeled fascicular groups. The only exception occurred when trying to selectively stimulate the vastus lateralis, in which the recruitment benefit was less than 10% before spillover exceeded 10% in two of the modeled fascicular groups. In these cases, 85% of axons that were activated due to spillover innervated the vastus medialis and vastus intermedius, which are synergists and functionally equivalent to vastus lateralis.

Similar results were found in choose-2 simulations. In 32 (76%) modeled fascicular groups, two contacts increased muscle selectivity compared to a single contact. On average, using a second contact increased muscle recruitment by 12.5% and resulted in a significantly greater selectivity in 28 (67%) modeled fascicular groups ($p \leq 0.05$). In the simulations where a single contact produced greater selectivity than two, there was a larger increase in recruitment costs than in recruitment benefits from the additional channel of stimulation.

In 90% of choose-2 simulations, one of the two selected contacts matched the single contact chosen in optimal choose-1 simulations. When a second contact was included in the choose-2 cases, it was most often either directly opposite or directly adjacent to the first contact. In 72% of simulations in which two contacts were chosen, the selected electrical contacts were located on both the upper and lower inner surfaces on opposite sides of the nerve. In 20% of the choose-2 simulations contacts were located adjacently with no more than 1 contact separating them. In 8% of simulations in which two contacts were chosen, contacts were neither opposite nor adjacent to each other. This occurred during simulations

targeting the sartorius in one of the cross sections, the fascicles for which were broadly spatially distributed rather than clustered.

C. Performance of Other Fine Configurations

Compared to the 22-contact FINE, all other electrode configurations produced a significantly lower average selectivity value for the electrode ($p \leq 0.05$) (Table IV). FINEs $8_{A/B}$ could selectively stimulate 60% of the muscles with a selectivity of at least 0.25. Similar to the 22-contact FINE, pure knee extension when seated was obtained by simultaneously stimulating a combination of two knee extensors to achieve a 40 Nm knee extension moment when using FINEs $8_{A/B}$ (Fig. 5). Selective stimulation of the sartorius and the pectineus muscles while in a standing posture resulted in a hip flexion moment of 5 ± 1 Nm and negligible knee extension moments. While in a seated posture, selective stimulation of the rectus femoris fascicles produced 11 ± 3 Nm of hip flexion moment and 15 ± 3 Nm of knee extension moment. In a standing posture, selective stimulation of the rectus femoris fascicles produced 13 ± 3 Nm of hip flexion moment and 24 ± 5 Nm of knee extension moment. Combined stimulation of all hip flexors with optimal selectivity in a standing posture produced 18 ± 4 Nm of hip flexion, which is 60% of the required hip flexion moment for gait. In eights-contact simulations, all eight contacts were chosen at least once to maximize selectivity.

The 11-contact FINEs (FINEs $11_{A/B}$) selectively activated a target muscle above threshold without activating any other muscle above threshold in at least 50% of simulations, producing a selectivity of at least 0.22. FINEs $11_{A/B}$ required the selective stimulation of all knee extensors to achieve 40 Nm of pure knee extension when in a seated posture. FINEs $11_{A/B}$ produced 16 ± 4 Nm of hip flexion when in a standing posture, or 53% of that required during gait. FINEs $6_{A/B}$ activated target muscles above threshold in at least 40% of simulations, producing a selectivity of at least 0.19. FINEs $6_{A/B}$ required the selective stimulation of all knee extensors to achieve 21 ± 11 Nm of pure knee extension when in a seated posture, or 53% of that required for the sit-to-stand transition. FINEs $6_{A/B}$ produced 14 ± 2 Nm of hip flexion when in a standing posture, or 47% of that required during gait. Centered contact (“C”) FINEs instead of the “A” or “B” configurations produced fewer simulations in which target muscles were activated above threshold. FINE 8_c activated target muscles above threshold with the 10% RC constraint in at least 50% of simulations, producing a selectivity of at least 0.28, depending on electrode opening height. Similarly, FINE 6_c activated target muscles above threshold with the 10% RC constraint in at least 40% of simulations, producing a selectivity of at least 0.19, depending on electrode opening height. The selectivity values obtained with six contacts FINEs were significantly less than those obtained with eight-contact FINEs for 22 (52%) of the modeled fascicle groups ($p \leq 0.05$).

A significantly greater selectivity and joint moment were achieved when the constraint that RC be less than 10% while maximizing muscle selectivity was removed (Fig. 6). With the constraint removed, the muscle selectivity for FINEs $8_{A/B}$ was at least 0.53. Knee extension with negligible hip flexion while in a seated posture was obtained by selectively stimulating the vastus intermedius or vastus medialis to achieve a 40 Nm knee extension moment when using FINEs $8_{A/B}$. Selective stimulation of the vastus lateralis also produced a knee extension moment exceeding 40 Nm but spillover resulted in a hip flexion moment of at least 12 Nm. Additionally, hip flexion when in a standing posture was obtained by selectively stimulating all hip flexors, producing a hip flexion moment exceeding 30 Nm but also producing knee extension moments.

Selectivity was correlated with electrode opening height. When selectivity was maximized without restricting recruitment costs, selectivity increased as electrode opening height

decreased for all FINE configurations. When the data were fit using linear regression, the slope of the fitted line was steeper for configurations with more contacts, ranging from 0.015 for six-contact FINEs to 0.041 for the 22-contact FINE. The associated R^2 values ranged between 0.57 and 0.96.

IV. Discussion

For a given opening height, FINEs with more contacts that were evenly distributed across the upper and lower inner surface of the FINE generally produced greater recruitment benefit, lower recruitment costs, and were able to selectively activate more muscles than FINEs with fewer contacts or the 11-contact FINEs in which contacts that were only positioned on one side of the electrode. With all contacts on only a single side, stimulation was selective for muscle that had fascicles on the same side of the nerve as the contacts but it was not selective for muscles that had fascicles located on the opposite side of the nerve. Therefore, although FINEs 11_{A/B} contained more contacts than FINEs 8_{A/B}, they achieved a lower average selectivity. For a given number of contacts, FINEs with a smaller opening height had greater selectivity than FINEs with a larger opening height. For a given electrode configuration, simultaneous use of two contacts produced higher selectivity when the stimulating contacts were located directly across from each other (top and bottom) or adjacent to each other. The 22-contact FINE attained greater selectivity than all other FINEs and, at a 1.4 mm opening height, was able to selectively stimulate every muscle above threshold without suprathreshold activation of any nontarget muscles above threshold in all tested nerve geometries.

While every FINE configuration was capable of stimulating every muscle, instances occurred in which the activation level within one or more nontarget muscles exceeded threshold before the target muscle exceeded threshold. Activation of a non-target muscle above threshold may be acceptable when the activated muscle is synergistic with the target muscle. For example, when targeting the vastus lateralis for knee extension, spillover to the vastus intermedius or vastus medialis, both of which extend the knee, will enhance the desired functional outcome by increasing the moment at the knee. In such cases, the “costs” in these simulations actually may be benefits. Activation of a non-target muscle above threshold also may be acceptable if the activated muscle does not alter the functional outcome significantly. When targeting a knee extensor, spillover to the pectineus may be acceptable because, even at full activation, the pectineus creates only minor hip flexion that may not be functionally noticeable.

In these simulations, we only considered the strictest definition of selectivity in determining our results. Activation of axons in the Medial Cutaneous and Saphenous sensory fascicles always contributed to recruitment costs and decreased selectivity. The neuroprosthesis user with a neurologically complete SCI is unlikely to experience discomfort from activated sensory fibers, so this assumption may be unnecessarily conservative. In a separate series of analyses in which activation of sensory fibers did not contribute to costs, selectivity was found to increase. Selectivity of the 22-contact FINE increased from at most 0.45, 0.52, and 0.74, depending on opening height, to 0.76, 0.88, and 0.68 for the vastus medialis, the sartorius, and the pectineus, respectively. Selectivity of FINEs 8_{A/B} increased from at most 0.16, 0.46, 0.59, depending on opening height, to 0.25, 0.79, and 0.66, respectively.

The strict optimization criterion presented was selected to guide design of the number and location of contacts on a FINE for selective stimulation. For some applications the optimization criterion is overly conservative. If RC were unconstrained, selectivity values increased by 0.30 ± 0.04 . The increase in selectivity was greatest for electrodes with fewer contacts. For example, selectivity increased by only 49% for the 22-contact FINE, but 162%

for FINE 6_C. However, in the unconstrained optimization, it was possible for the activation level of a non-target muscle to exceed that of the target muscle. This occurred when the nontarget muscle contributed only a small percentage to the total recruitment costs.

The data presented in this paper indicate that even under a strict optimization criterion, selective stimulation of the femoral nerve is possible and can produce knee extension moments that are sufficient for the sit-to-stand transition and hip flexion moments that are nearly sufficient for gait. While the performance of the 22-contact FINE was superior to other electrode configurations tested, available implantable stimulators for a lower extremity neural prosthesis generally are limited in the number of channels available for stimulation for the femoral nerve. These models indicate 8 channels will be sufficient for standing and potentially gait.

Simulations suggest that carousel stimulation may be possible [31]. By interleaving activation of some but not all of the muscles to create the required 40 Nm knee extension moment, nonactive muscles are given some amount of time to rest. This should delay the onset of fatigue and extend the duration of time an activity can be performed.

There are several assumptions in this model. To convert the fraction of activated axons to muscle force, a simple assumption of equal axonal fraction to percent muscle activation was used. This is known not to be true as activation of larger diameter axons activate larger motor units and, therefore, larger contractile forces than activation of smaller diameter axons [32]. Because these models do not account for the diameter of the activated axon they under predict the expected joint moment, particularly at lower stimulus levels.

Another assumption was that the costs of all muscles should be equally weighted when calculating selectivity. However, the maximum moments that each muscle produces are not equal. If the goal of the simulations is to maximize the percentage of a muscle that is selectively activated, then the procedures detailed in this study are appropriate. However, if the goal of the simulations is to maximize the functional response of a system to stimulation, then the costs of each muscle recruited should be weighted by its contribution to the functional output.

The volume between the nerve and the inner surface of the electrode as well as that immediately surrounding the electrode was modeled as saline. This is a reasonable assumption when modeling the intraoperative environment, in which the cavity surrounding the exposed femoral nerve often fills with fluid. In a separate series of simulations, the electrode was sheathed in 0.25 mm of an encapsulation tissue that had a conductivity of 0.1 S/m [33]–[35]. While the extracellular potential differed from models that did not contain encapsulation, the normalized field distribution along axons were nearly identical, differing by less than 1% along the portion of the axon closest to a contact. Therefore, it is unlikely that the inclusion of encapsulation in these models will change selectivity or their associated joint moments significantly.

The actual performance of a FINE will depend on the cross-sectional morphology of the nerve. However, this study shows that electrode performance is consistent across three different cross sections. Significant modifications of the results are not expected if the electrode location is varied between the inguinal ligament and the first branch point of the nerve because it has been shown that fascicles do not migrate substantially or deviate from a nearly straight path through this region of the nerve [16]. The presented methods can be applied to other nerve targets, but require cross-sectional morphology of the specific nerve to develop realistic models. These model techniques are valuable tools in the translational process for developing a functional neural prosthesis.

V. Conclusion

This simulation study suggests that selective stimulation of the six muscles innervated by the common femoral nerve is possible using a Flat Interface Nerve Electrode. A 22-contact FINE can selectively activate each muscle within the femoral nerve and produce moments that are sufficient for the sit-to-stand transition by activating individual muscles or a combination of agonists. Selective stimulation of the femoral nerve is predicted to produce 70% of the hip flexion moment needed during gait. Selectivity, and consequently, joint moments are increased using two stimulating contacts per muscle.

While the best electrode configuration predicted is the 22-contact FINE, FINEs $8_{A/B}$ produce sufficient selectivity with fewer contacts for a variety of geometries. An eight-contact FINE can be expected to selectively stimulate at least 60% of the muscles above threshold without stimulating any other muscle above threshold. Further, these models suggest that selective stimulation with an eight-contact FINE will produce a sufficient knee extension moment for the sit-to-stand transition and 60% of the hip flexion moment needed during gait in all femoral nerve geometries studied. The nerves modeled in this study were similar in size and shape, but had a large variability in fascicular distributions. Because the selectivity obtained with an eight contact FINE was sufficient across all simulated nerves, this study suggests that a single electrode design should operate well across a population with a large range of variance in the size, location, and number of fascicles within the nerve. The eight-contact FINE represents an acceptable tradeoff between the competing design goals of minimizing contacts and maximizing muscle selectivity for functional outcome. Prior experiments in animals showed the selective stimulation capabilities of the FINE. This simulation study of the FINE on human femoral nerves is an important step in the design process prior to clinical implementation. An eight-contact FINE is expected to achieve sufficient selectivity to produce moments required for a standing and gait neuroprosthesis.

Acknowledgments

The project described was supported in part by Grant Number R01-EB001889-01 from the National Institute of Biomedical Imaging and Bioengineering (NIBIB). Its contents are solely the responsibility of the authors and do not necessarily represent the official views of the NIBIB. This work was also supported in part by the U.S. Department of Graduate Assistance in Areas of National Need Fellowship, in part by the Ohio Supercomputer Center, in part by the Advanced Platform Technology Center of the Rehabilitation Research and Development Service of the U.S. Department of Veterans Affairs under Grant C3819C, and in part by the Ohio Third Frontier Innovation Incentive Fellowship.

References

1. Data provided by the national spinal cord injury statistical center. Dept. Physical Medicine and Rehabilitation, Univ. Alabama; Birmingham: [Online]. Available: <http://main.uab.edu/show.asp?durki=10766>
2. Ergas Z. Spinal cord injury in the united states: A statistical update. *Cent Nerv Syst Trauma* 1985;2:19–32. [PubMed: 4092238]
3. Nobunaga AI, Go BK, Karunas RB. Recent demographic and injury trends in people served by the model spinal cord injury care systems. *Arch Phys Med Rehabil* 1999;80:1372–1382. [PubMed: 10569430]
4. Triolo R, Wibowo M, Uhlir J, Kobetic R, Kirsch R. Effects of stimulated hip extension moment and position on upper-limb support forces during fns-induced standing—a technical note. *J Rehab Res Develop* 2001;38:545–555.
5. Triolo RJ, Bevelheimer T, Eisenhower G, Wormser D. Inter-rater reliability of a clinical test of standing function. *J Spinal Cord Med* 1995;18:14–22. [PubMed: 7640969]
6. Triolo, R.J.; Kobetic, R.; Betz, R. Standing and walking with fns: Technical and clinical challenges. In: Harris, G., editor. *Human Motion Analysis*. New York: IEEE Press; 1996. p. 318-350.

7. Uhler JP, Triolo RJ, Davis JA Jr, Bieri C. Performance of epimysial stimulating electrodes in the lower extremities of individuals with spinal cord injury. *IEEE Trans Neural Syst Rehabil Eng Jun*; 2004 12(2):279–287. [PubMed: 15218941]
8. Tarler MD, Mortimer JT. Selective and independent activation of four motor fascicles using a four contact nerve-cuff electrode. *IEEE Trans Neural Syst Rehabil Eng Jun*;2004 12(2):251–257. [PubMed: 15218938]
9. Tyler DJ, Durand DM. Functionally selective peripheral nerve stimulation with a flat interface nerve electrode. *IEEE Trans Neural Syst Rehabil Eng Dec*;2002 10(4):294–303. [PubMed: 12611367]
10. Leventhal DK, Durand DM. Subfascicle stimulation selectivity with the flat interface nerve electrode. *Ann Biomed Eng Jun*;2003 31(6):643–652. [PubMed: 12797613]
11. Creasey G, Elefteriades J, DiMarco A, Talonen P, Bijak M, Girsch W, Kantor C. Electrical stimulation to restore respiration. *J Rehab Res Develop* 1996;33:123–132.
12. Uhler JP, Triolo RJ, Kobetic R. The use of selective electrical stimulation of the quadriceps to improve standing function in paraplegia. *IEEE Trans Rehabil Eng Dec*;2000 8(4):514–522. [PubMed: 11204043]
13. Kagaya H, Shimada Y, Ebata K, Sato M, Sato K, Yukawa T, Obinata G. Restoration and analysis of standing-up in complete paraplegia utilizing functional electrical stimulation. *Arch Phys Med Rehabil* 1995;76:876–881. [PubMed: 7668962]
14. Winter, DA. *Biomechanics of Motor Control and Human Gait*. Waterloo, ON, Canada: Univ. Waterloo Press; 1991.
15. Piazza SJ, Delp SL. The influence of muscles on knee flexion during the swing phase of gait. *J Biomech Jun*;1996 29(6):723–733. [PubMed: 9147969]
16. Gustafson, KJ.; Neville, JJ.; Syed, I.; Davis, JA.; Triolo, RJ. Fascicular anatomy human femoral nerve: Implications for neural prostheses utilizing nerve cuff electrodes. *Proc 34th Annual NIH Neural Prosthesis Workshop*; 2003.
17. Grinberg, Y.; Schiefer, MA.; Tyler, DJ.; Gustafson, KJ. Effects of fascicle size and perineurial thickness on stimulation selectivity. *Proc. BMES Annu. Fall Meeting*; 2007.
18. Tyler DJ, Durand DM. Chronic response of the rat sciatic nerve to the flat interface nerve electrode. *Ann Biomed Eng Jun*;2003 31(6):633–642. [PubMed: 12797612]
19. Behse F. Morphometric studies on the human sural nerve. *Acta Neurol Scand Suppl* 1990;132:1–38. [PubMed: 2239145]
20. Garven HS, Gairns FW, Smith G. The nerve fibre populations of the nerves of the leg in chronic occlusive arterial disease in man. *Scott Med J* 1962;7:250–265. [PubMed: 13897116]
21. McIntyre CC, Richardson AG, Grill WM. Modeling the excitability of mammalian nerve fibers: Influence of afterpotentials on the recovery cycle. *J Neurophysiol* 2002;87:995–1006. [PubMed: 11826063]
22. Richardson AG, McIntyre CC, Grill WM. Modelling the effects of electric fields on nerve fibres: Influence of the myelin sheath. *Med Biol Eng Comput Jul*;2000 38(4):438–446. [PubMed: 10984943]
23. Choi AQ, Cavanaugh JK, Durand DM. Selectivity of multiple-contact nerve cuff electrodes: A simulation analysis. *IEEE Trans Biomed Eng Feb*;2001 48(2):165–172. [PubMed: 11296872]
24. Tarler MD, Mortimer JT. Comparison of joint torque evoked with monopolar and tripolar-cuff electrodes. *IEEE Trans Neural Syst Rehabil Eng Sep*;2003 11(3):227–235. [PubMed: 14518785]
25. Delp, SL. *Surgery Simulation: A Computer Graphics System to Analyze and Design Musculoskeletal Reconstructions of the Lower Extremity*. Stanford, CA: Stanford Univ. Press; 1990.
26. Delp SL, Loan JP, Hoy MG, Zajac FE, Topp EL, Rosen JM. An interactive graphics-based model of the lower extremity to study orthopaedic surgical procedures. *IEEE Trans Biomed Eng Aug*; 1990 37(8):757–767. [PubMed: 2210784]
27. Wickiewicz TL, Roy RR, Powell PL, Edgerton VR. Muscle architecture of the human lower limb. *Clin Orthop* 1983:275–283. [PubMed: 6617027]
28. Friederich JA, Brand RA. Muscle fiber architecture in the human lower limb. *J Biomech* 1990;23(1):91–95. [PubMed: 2307696]

29. Brand RA, Pedersen DR, Friederich JA. The sensitivity of muscle force predictions to changes in physiologic cross-sectional area. *J Biomech* 1986;19:589–596. [PubMed: 3771581]
30. Johnson, RA.; Wichern, DW. *Applied Multivariate Statistical Analysis*. 5. Englewood Cliffs, NJ: Prentice-Hall; 2002.
31. Koller R, Girsch W, Huber L, Rab M, Stoehr HG, Schima H, Rokitansky AM, Losert UM, Wolner E. Influence of different conditioning methods on force and fatigue resistance in chronically stimulated skeletal muscles. *Pacing Clin Electrophysiol* 1996;19:222–230. [PubMed: 8834692]
32. Enoka RM, Fuglevand AJ. Motor unit physiology: Some unresolved issues. *Muscle Nerve* 2001;24:4–17. [PubMed: 11150961]
33. Butson CR, Maks CB, McIntyre CC. Sources and effects of electrode impedance during deep brain stimulation. *Clin Neurophysiol* 2006;117:447–454. [PubMed: 16376143]
34. Grill WM, Mortimer JT. Electrical properties of implant encapsulation tissue. *Ann Biomed Eng* Jan;1994 22(1):23–33. [PubMed: 8060024]
35. Miocinovic S, Parent M, Butson CR, Hahn PJ, Russo GS, Vitek JL, McIntyre CC. Computational analysis of subthalamic nucleus and lenticular fasciculus activation during therapeutic deep brain stimulation. *J Neurophysiol* 2006;96:1569–1580. [PubMed: 16738214]
36. Gray, H. *Anatomy of the Human Body*. Philadelphia, PA: Lea Febiger; 1918.

Biographies



Matthew A. Schiefer (S'02) received the B.E. degree in biomedical engineering from Vanderbilt University, Nashville, TN, in 2001. In 2003, he received the M.S. degree in biomedical engineering from Case Western Reserve University, Cleveland, OH, for work involving computer modeling of the effects of electrical stimulation on the human retina. He is currently pursuing the Ph.D. degree in the Biomedical Engineering Department, Case Western Reserve University.

His research interests include neural modeling, finite element modeling, and restoration of function through electrical stimulation.

Mr. Schiefer received an innovation incentive fellowship by Case Western Reserve University in conjunction with the Ohio Third Frontier project in 2006 and again in 2007.



Ronald J. Triolo (S'78–M'86) received the doctoral degree in biomedical engineering from Drexel University, Philadelphia, PA, in 1986 after receiving M.S. degrees in both biomedical engineering and electrical engineering in 1982 and 1984, respectively. His doctoral work involved the design and clinical testing of an actively powered and myoelectrically controlled above knee prosthesis for transfemoral amputees.

He is the Director of the Advanced Platform Technology Center of Excellence of the Rehabilitation Research and Development Service, Department of Veterans Affairs. A tenured Associate Professor of Orthopaedics and Biomedical Engineering at Case Western Reserve University, he is also a Member of the Bioscientific Staff of MetroHealth Medical Center in Cleveland, OH. He directs the Motion Study Laboratory of the Cleveland FES

Center, a national center of excellence in functional electrical stimulation and research consisting of Case Western Reserve University, MetroHealth Medical Center, and the Louis Stokes Cleveland Department of Veterans Affairs Medical Center. His research interests include the development and clinical application of neural prostheses and restorative technologies, biomechanics and the control of movement, rehabilitation engineering, analysis of human gait and posture, and the assessment of assistive technology. He serves on the editorial board of *Journal of Rehabilitation Research & Development*.

Dr. Triolo is the recipient of the Maurice Saltzman Award for clinical excellence from the Mt. Sinai Foundation and a recipient of a Senior Research Career Scientist award from the Department of Veterans Affairs. He is a member of the Rehabilitation Engineering Society of North America, American Spinal Injury Society, and International Functional Electrical Stimulation Society and serves on the editorial board of the *IEEE Transactions on Neural Systems and Rehabilitation Engineering*.



Dustin J. Tyler (S'92–M'99) received the B.S. degree in electrical engineering from Michigan Technological University, Houghton, in 1992 and the Ph.D. degree in biomedical engineering from Case Western Reserve University, Cleveland, OH, in 1999.

From 1998 to 2002, he worked in research and development in the industrial sector designing functional electrical stimulation products for spinal cord injured and stroke patients. He joined the faculty of the Biomedical Engineering Department, Case Western Reserve University, as a tenure-track Assistant Professor in August 2004. He is also currently a Research Scientist at the Cleveland Functional Electrical Stimulation Center of Excellence and Associate Director of the Advanced Platform Technology Center of Excellence, both at the Cleveland Department of Veteran's Affairs Medical Center. His

research interests include clinical implementation of neural interfaces; neuromimetic devices; neural modeling; neuroprostheses for restoration of lost function in neurologically impaired individuals; and neuroprostheses for head and neck applications.

Dr. Tyler is a member the Materials Research Society, Biomedical Engineering Society, AAAS, and Tau Beta Pi.

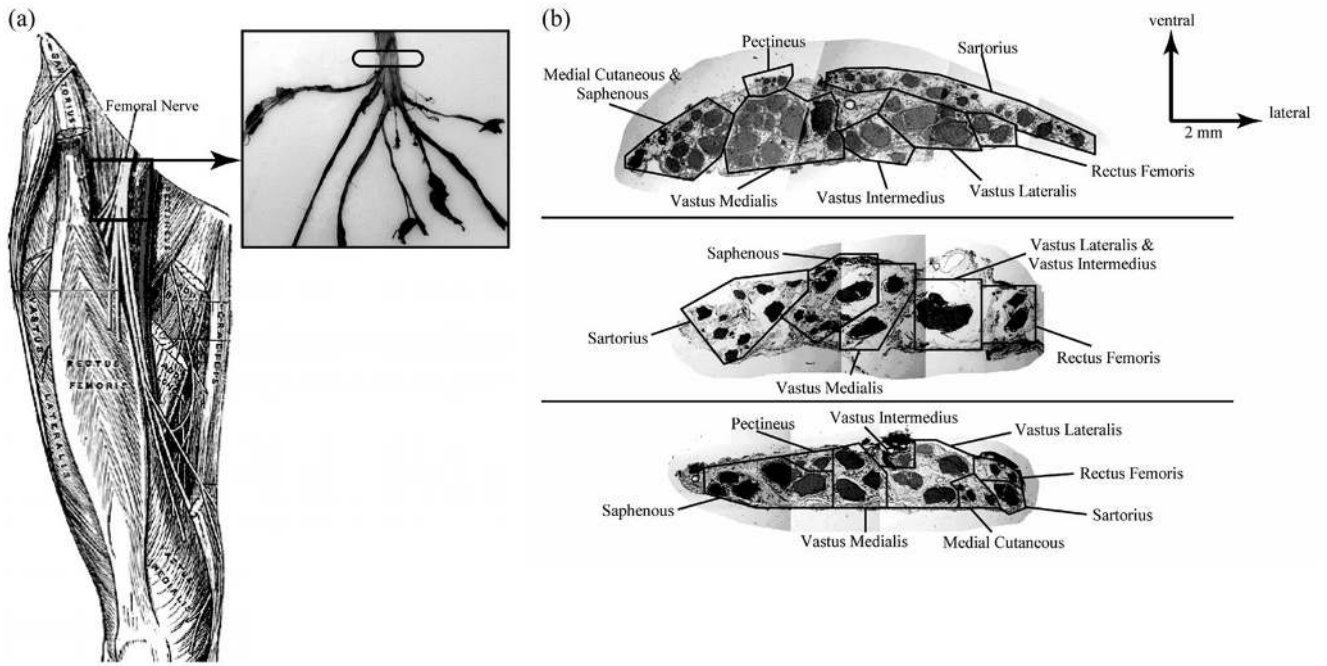


Fig. 1. (a, left) Target location for FINE placement is along the femoral nerve distal to the inguinal ligament and proximal to nerve branching [36]. (a, right) Representative femoral nerve taken from a cadaver. The target location for FINE placement and selective activation of all muscles innervated by the femoral nerve is marked with a translucent ellipse. (b) Cross sections of the three nerves used to produce the FEM models [16]. Fascicles innervating the same muscle were noted.

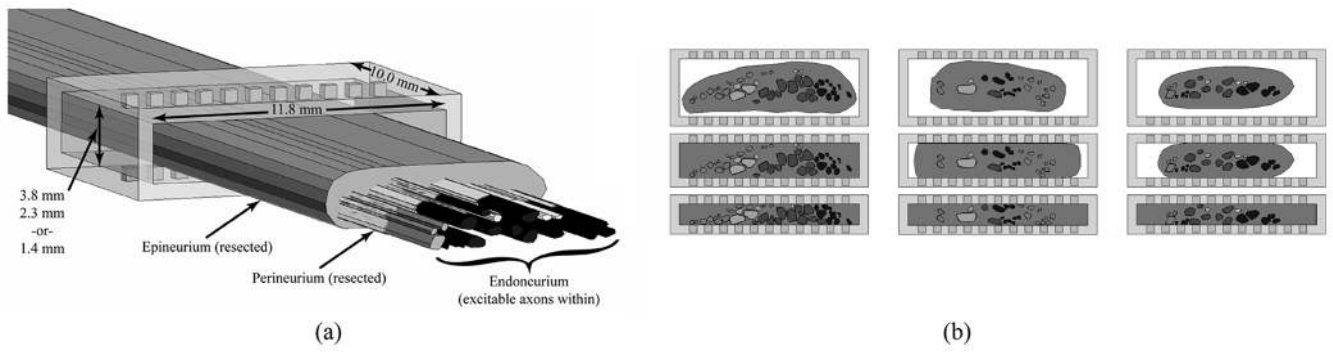


Fig. 2.
 (a) Three-dimensional FEM model of the nerve surrounded by a 22-contact flat interface nerve electrode (FINE). The epineurium and perineurium have been hidden to show the endoneurium inside. The opening height, width, and length of the FINE are shown. (b) Two-dimensional view of the FEM model cross sections based on three excised human femoral nerves (columns) at the three FINE opening heights (rows) of 3.8, 2.3, and 1.4 mm.

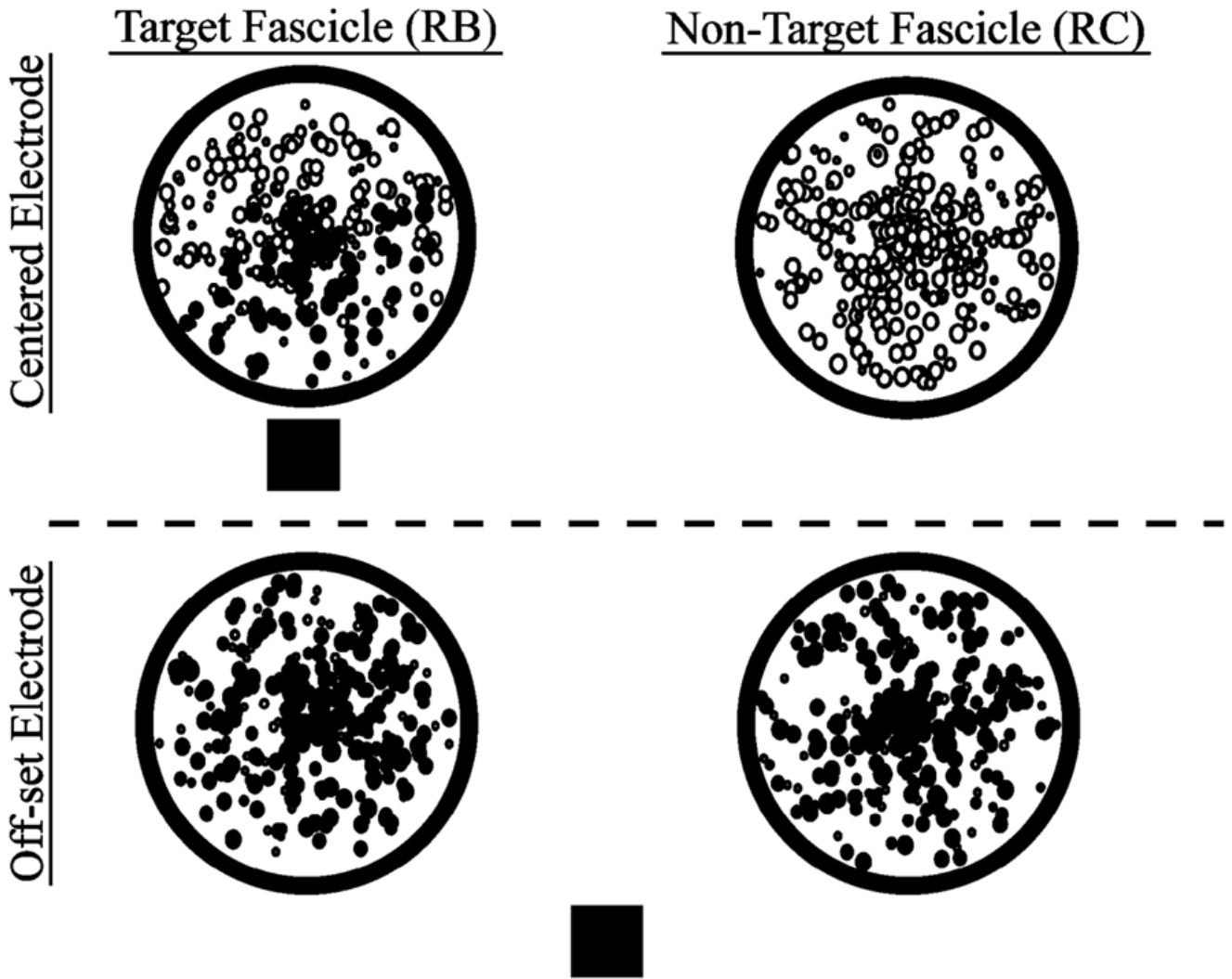


Fig. 3. To calculate selectivity, the fraction of axons that were activated in non-target fascicles (RC) was subtracted from the fraction of axons that were activated in target fascicles (RB). Axons, represented by the circles inside the fascicles, were randomly distributed. The size of the representative circle is proportional to the randomly assigned diameter of the axon. Although circles overlap due to their size, axons did not. Solid circles represent activated axons. The square represents the stimulating electrode.

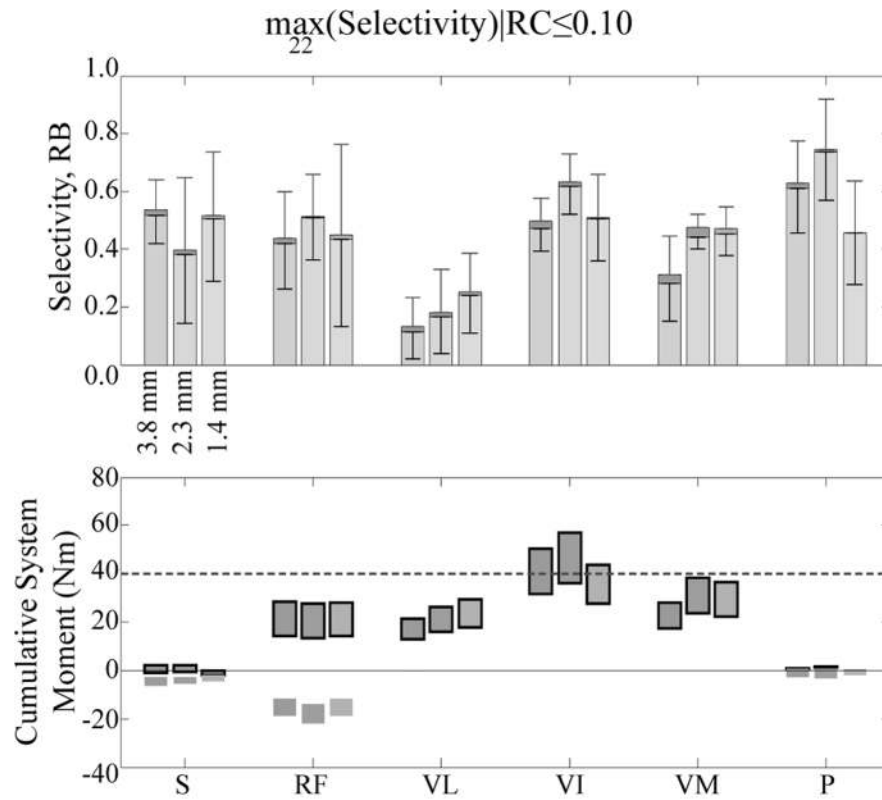


Fig. 4. (a) Muscle recruitment (upper stacked bars) and selectivity (lower stacked bars) averaged across all cross sections exceeded threshold for each muscle at each opening height using the 22-contact FINE when costs were limited to 10% or less. (b) Cumulative knee (outlined) and hip moment ranges resulting from the activation of muscles at the levels shown in (a) indicated that sufficient knee extension moment could be obtained for the sit-to-stand transition and that 70% of hip flexion moment required for gait could be achieved. Fascicular groups are sartorius (S), rectus femoris (RF), vastus lateralis (VL), vastus intermedius (VI), vastus medialis (VM), and pectineus (P).

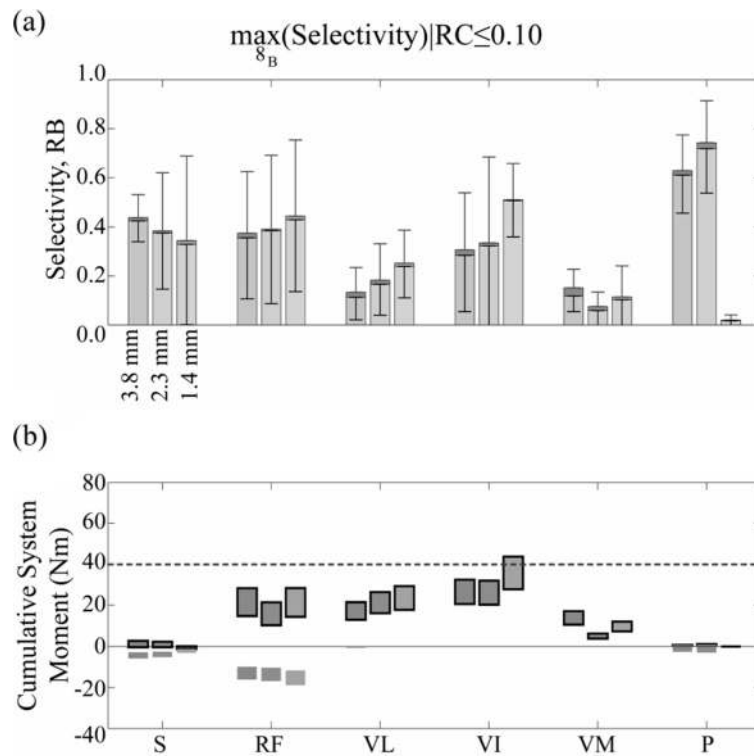


Fig. 5. (a) Muscle recruitment (upper stacked bars) and selectivity (lower stacked bars) averaged across all cross sections exceeded threshold for each muscle at each opening height using an eight-contact FINE when costs were limited to 10% or less except VI and P. (b) Cumulative knee (outlined) and hip moment ranges resulting from the activation of muscles at the levels shown in (a) indicated that sufficient knee extension moment could be obtained for the sit-to-stand transition and that 60% of hip flexion moment required for gait could be achieved during simultaneous stimulation of agonists. Fascicular groups were defined in Fig. 4.

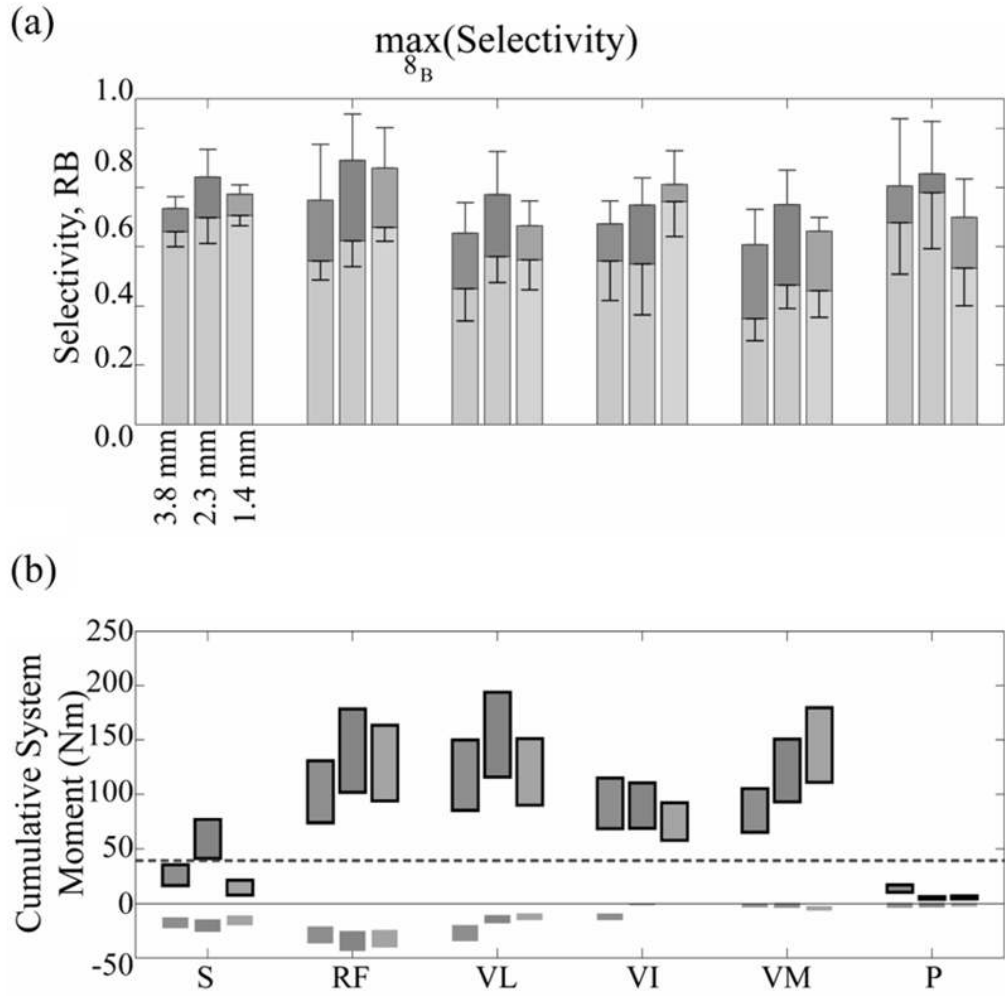


Fig. 6. (a) Average selectivity obtained in all models for each fascicle group at given opening heights for fine 8_b choose-1. Stacked upper bar is recruitment benefit (range: 0 to 1), lower bar is selectivity (range: -1 to 1). (b) Cumulative moment range arising from moment ranges produced by targeted activation of each muscle. Outlined moments were knee moments or were otherwise hip moments. Fascicular groups were defined in Fig. 4.




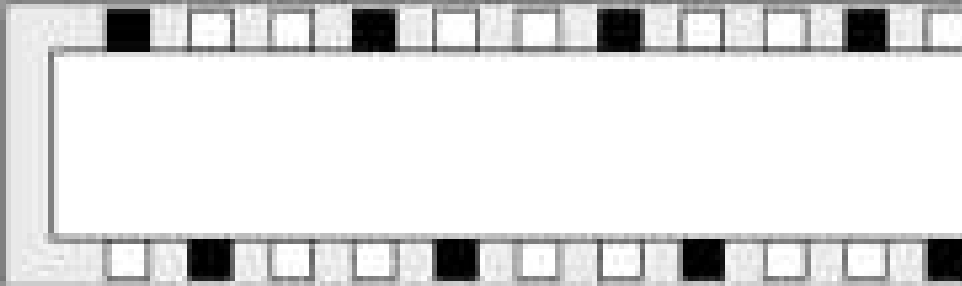

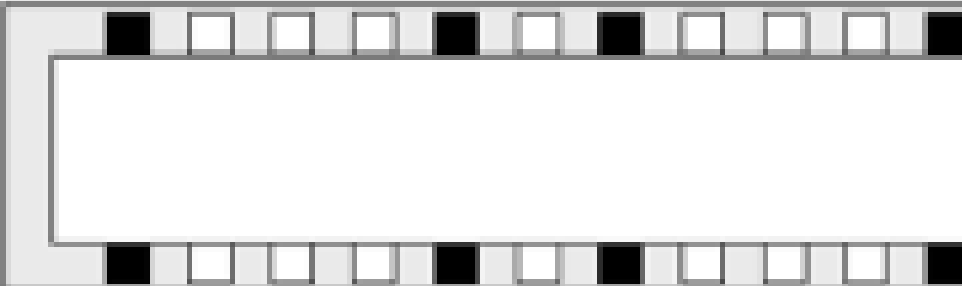
TABLE I

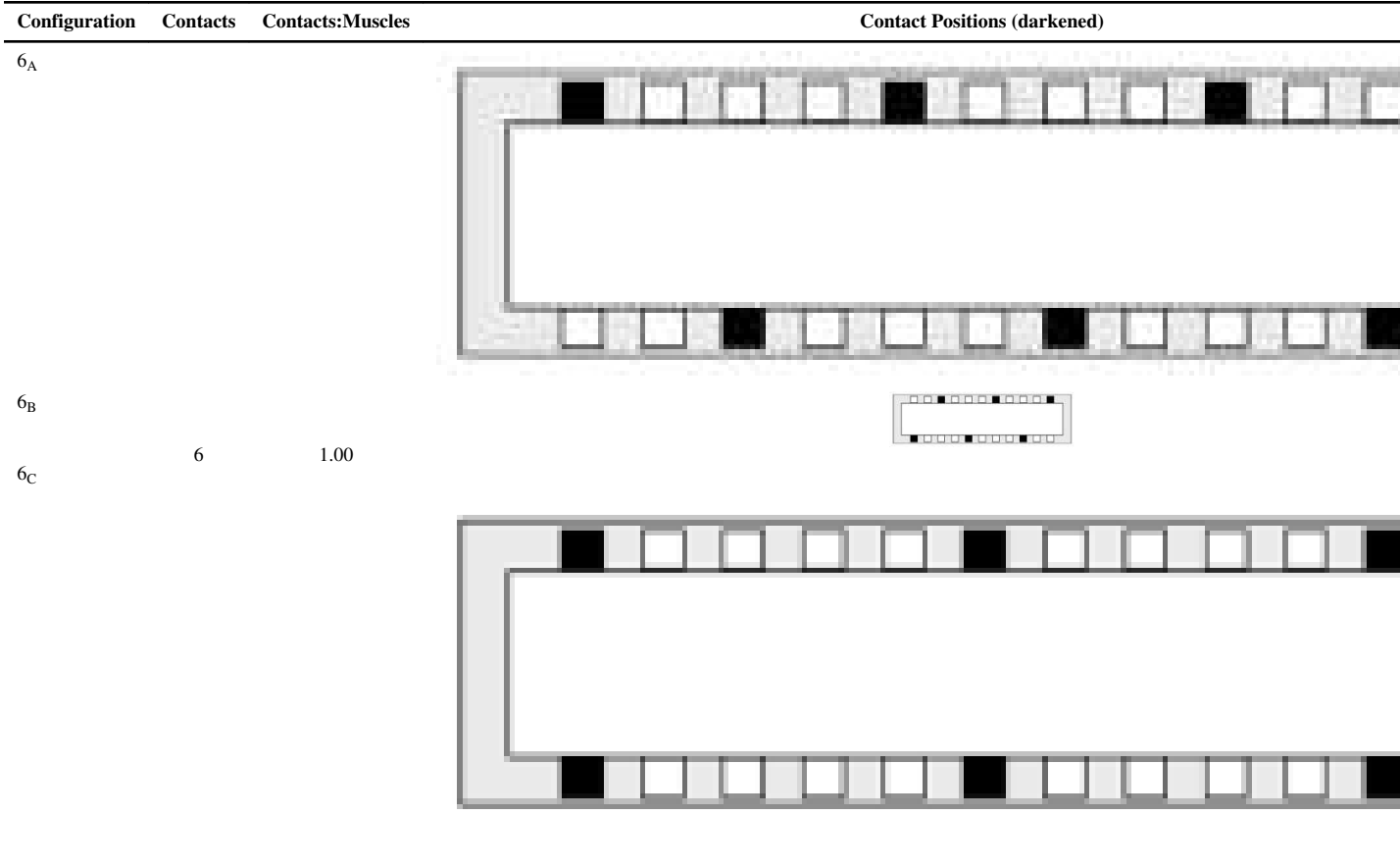
Electrical Properties of Neural Tissue [23]

Material	Conductivity(S/m)		
	x-direction (transverse)	y-direction (transverse)	z-direction (parallel)
Endoneurium	0.083	0.083	0.571
Perineurium	0.002	0.002	0.002
Epineurium	0.083	0.083	0.083
Saline	2.000	2.000	2.000

TABLE II

Simulated Electrode Configurations

Configuration	Contacts	Contacts:Muscles	Contact Positions (darkened)
22	22	3.67	
11 _A	11	1.83	
11 _B			
8 _A	8	1.33	
8 _B			
8 _C			



“B” versions were mirror images of “A” versions.

TABLE III

Simm-Predicted Range of Joint Moments (NM)

Innervated Muscle	Knee	Hip
Vastus Lateralis	70 to 116	0
Vastus Intermedius	53 to 82	0
Vastus Medialis	47 to 77	0
Rectus Femoris	24 to 51	-42 to -26
Sartorius	-4 to 0	-9 to -4
Pectineus	0	-4 to 1

Moments are expected during maximal muscle contraction in either the sitting or standing posture. Extension: >0; Flexion: <0

TABLE IV

Simulated Selectivity Values

Target Fascicular Group	FINE Opening Height		
	3.8 mm	2.3 mm	1.4 mm
22-contact FINE			
Sartorius	0.52±0.06	0.38±0.04	0.51±0.05
Rectus Femoris	0.42±0.05	0.51±0.06	0.44±0.05
Vastus Lateralis	0.11±0.05	0.17±0.05	0.24±0.12
Vastus Intermedius	0.47±0.08	0.62±0.10	0.51±0.15
Vastus Medialis	0.28±0.04	0.44±0.04	0.45±0.05
Pectineus	0.61±0.07	0.74±0.08	0.46±0.18
FINE11 _{A/B}			
Sartorius	0.36±0.21	0.35±0.26	0.42±0.30
Rectus Femoris	0.29±0.24	0.36±0.27	0.39±0.33
Vastus Lateralis	0.07±0.08	0.09±0.12	0.16±0.12
Vastus Intermedius	0.24±0.25	0.31±0.32	0.25±0.28
Vastus Medialis	0.19±0.14	0.25±0.21	0.30±0.17
Pectineus	0.31±0.33	0.37±0.40	0.23±0.27
FINE 8 _{A/B}			
Sartorius	0.46±0.11	0.36±0.23	0.40±0.27
Rectus Femoris	0.32±0.24	0.33±0.30	0.40±0.33
Vastus Lateralis	0.07±0.08	0.10±0.11	0.16±0.12
Vastus Intermedius	0.27±0.17	0.31±0.28	0.25±0.28
Vastus Medialis	0.16±0.14	0.16±0.18	0.12±0.13
Pectineus	0.58±0.13	0.59±0.22	0.24±0.26
FINE 8 _C			
Sartorius	0.40±0.12	0.37±0.23	0.33±0.33
Rectus Femoris	0.28±0.24	0.27±0.30	0.35±0.37
Vastus Lateralis	0.02±0.03	0.03±0.05	0.00±0.00
Vastus Intermedius	0.40±0.12	0.38±0.29	0.51±0.15
Vastus Medialis	0.20±0.17	0.12±0.17	0.14±0.15
Pectineus	0.56±0.10	0.47±0.18	0.46±0.18
FINE 6 _{A/B}			
Sartorius	0.33±0.15	0.35±0.25	0.35±0.35
Rectus Femoris	0.26±0.21	0.30±0.28	0.36±0.33
Vastus Lateralis	0.00±0.00	0.02±0.04	0.00±0.00
Vastus Intermedius	0.22±0.21	0.19±0.28	0.25±0.28
Vastus Medialis	0.14±0.14	0.10±0.13	0.12±0.13
Pectineus	0.44±0.26	0.28±0.24	0.23±0.27

Target Fascicular Group	FINE Opening Height		
	3.8 mm	2.3 mm	1.4 mm
FINE 6 _C			
Sartorius	0.40±0.12	0.37±0.23	0.33±0.33
Rectus Femoris	0.28±0.24	0.27±0.30	0.35±0.37
Vastus Lateralis	0.00±0.00	0.00±0.00	0.00±0.00
Vastus Intermedius	0.22±0.24	0.30±0.032	0.00±0.00
Vastus Medialis	0.21±0.17	0.30±0.22	0.45±0.08
Pectineus	0.00±0.00	0.00±0.00	0.00±0.00

Selectivity and standard deviations obtained during stimulation via a single contact (“choose-1”) in which non-target muscles could not be activated above threshold (0.10). Values were obtained by averaging the five randomized populations for each cross-section across the three unique cross-sections. A/B data are averaged from the individual A and B configurations. Black cells indicate fascicle groups for which costs exceeded threshold before benefits exceeded threshold.